

# A MINIMAL CONTROL SCHEMA FOR GOAL-DIRECTED ARM MOVEMENTS BASED ON PHYSIOLOGICAL INTER-JOINT COUPLINGS

Till Bockemühl<sup>1</sup> and Volker Dürr<sup>1,2</sup>

<sup>1</sup>Dept. of Biological Cybernetics, <sup>2</sup>Cognitive Interaction Technology - Center of Excellence, CITEC  
University of Bielefeld, PO Box 100131, 33501 Bielefeld, Germany

Keywords: Motor control, Motor synergies.

Abstract: Substantial evidence suggests that nervous systems simplify motor control of complex body geometries by use of higher level functional units, so called motor primitives or synergies. Although simpler, such high level functional units still require an adequate controller. In a previous study, we found that kinematic inter-joint couplings allow the extraction of simple movement synergies during unconstrained 3D catching movements of the human arm and shoulder girdle. Here, we show that there is a bijective mapping between movement synergy space and 3D Cartesian hand coordinates within the arm's physiological working range. Based on this mapping, we propose a minimal control schema for a 10-DoF arm and shoulder girdle. All key elements of this schema are implemented as artificial neural networks (ANNs). For the central controller, we evaluate two different ANN architectures: a feed-forward network and a recurrent Elman network. We show that this control schema is capable of controlling goal-directed movements of a 10-DoF arm with as few as five hidden units. Both controller variants are sufficient for the task. However, end-point stability is better in the feed-forward controller.

## 1 INTRODUCTION

The complex biomechanics of limbs like the primate arm facilitates the generation of a remarkable variety of dexterous and context-dependent behaviors. However, the large number of degrees of freedom (DoFs), e.g. ten DoFs of the human arm and shoulder girdle, complicates the required neural control. This issue is known as motor redundancy problem (Bernstein, 1967).

Central nervous systems (CNS) seem to easily overcome this problem. One proposed mechanism used by the CNS for the solution of the redundancy problem is the combination of several DoFs into a small set of higher level functional control units, typically referred to as movement synergies or primitives. There is substantial evidence that this general concept is realized in vertebrate nervous systems in one way or another (for reviews see Flash and Hochner, 2005, and Ting and McKay, 2007). Because the complexity of the control problem depends on the number of controlled variables, these synergies can simplify the control of the limb. Here, we propose and evaluate a synergy-based and

closed-loop control schema that can be implemented as a modular artificial neural network.

Classical studies on human reaching movements tended to search for global optimization parameters like speed (Atkeson and Hollerbach, 1985), jerk (Flash and Hogan, 1985), or torque change (Uno, et al., 1989). Most, if not all of these studies were based on well-controlled but strongly constrained movement paradigms, such as center-out tasks with planar movements and fixed shoulder position. Although these studies identified movement invariants, they did not specify models of how the brain could use them to overcome the problem of redundancy. Furthermore, these invariants are based on predictive strategies, i.e. global parameters that are optimized offline and prior to the actual movement. In these strategies sensory feedback during an ongoing movement plays only a minor role.

In contrast, current concepts of goal-directed behavior favor prospective strategies that (a) explicitly take into account sensory feedback during ongoing behavior and (b) define motor goals in a task space that is then mapped to motor output (Todorov, 2004). Both of these aspects are realized

in the approach we propose here: (a) It relies on continuous sensory feedback and (b) exploits a small set of movement synergies, which can be viewed as a set of elementary motor tasks as each synergy by itself defines a valid movement.

In a previous experiment (Bockemühl, et al., 2010) we studied natural and unconstrained arm movements during a catching task in a large portion of the arm's workspace and recorded 10-D joint angular time courses thereof. Using principal components analysis (PCA) for synergy extraction we found that the distribution of recorded postures that occur during movements can be described efficiently by linear combinations of a set of three inter-joint couplings. We also found that the individual contributions of these kinematic synergies varied systematically with catching position in external (Cartesian) hand coordinates. Together with the fact that three is the minimum number of synergies for control of end-effector position in 3D, this suggests that neural control of arm movements may exploit a simple mapping between synergy space and Cartesian space. Here, we show that the mapping between synergy space and hand position is bijective within a large physiological working range.

Based on the three movement synergies that capture natural inter-joint couplings, we propose a simple closed-loop control schema for a 10-DoF limb consisting of shoulder girdle, upper and lower arm and hand. All elements of this schema are implemented as ANNs. We evaluate two alternative ANN variants as central controller: a multilayer feed-forward network and a recurrent Elman network.

We show that both controller variants we examine here can generate physiological trajectories of goal-directed reaching movements, similar to those found experimentally. The networks are also capable of generating reaching movements towards novel targets, as well as smoothly interpolating between two different movements. Internal recurrence in the Elman controller improves learning of physiological training data. In contrast to the multilayer feed-forward network, however, the Elman controller shows a tendency to drift and fails to maintain a resting posture that keeps the hand at the target position.

## 2 MATERIAL AND METHODS

### 2.1 Kinematic Model

We use a 10 DoF kinematic model of the human

upper limb, i.e., arm and shoulder girdle. The model comprises 4 segments corresponding to a collarbone that moves the shoulder joint with 3 DoFs, a shoulder joint that moves the upper arm with 3 DoFs, an elbow and lower arm with 2 DoFs, and a hand with 2 DoFs. Segment lengths within the model are adjusted individually for each one of nine recorded human subjects (Bockemühl, et al., 2010). Consequently, each set of 10 joint angles is equivalent to a unique posture, and standard forward kinematics can be used to calculate the hand position (end-effector).

### 2.2 Inter-joint Coupling Gives Rise to Movement Synergies

The inter-joint couplings found in natural human, one-handed catching movements are equivalent to the first three principal components (PCs) of 10-D arm postures (Bockemühl, et al., 2010). Each PC constitutes a movement synergy so that each posture can be described by a linear combination of the mean posture of the original data set and a weighted sum of three movement synergies. Because the kinematic model, mean posture, and movement synergies are fixed for a given subject, any hand position in 3-D Cartesian space can solely be described by a 3-D vector of scores that scale the contribution of each synergy (see Equation 1).

$$\mathbf{p}(t) = \mathbf{m} + \sum_{i=1}^3 s_i(t) \mathbf{v}_i \quad (1)$$

Here,  $\mathbf{p}(t)$  represents a 10-D posture at time  $t$ ,  $\mathbf{m}$  is the mean posture,  $s_i(t)$  is the score of the posture  $\mathbf{p}(t)$  on the  $i^{\text{th}}$  synergy, and  $\mathbf{v}_i$  is the  $i^{\text{th}}$  synergy. Modulating the scores in a target-dependent manner therefore generates target-dependent hand trajectories.

### 2.3 Control Structure and Artificial Neural Networks

Given the current hand position and a target position, e.g., the position of a ball to be caught, our main goal is to generate an appropriate time series of postures that moves the hand from its current position to the target. Appropriate means that hand trajectories should match the measured ones. Since natural movements are marked by substantial inter-joint couplings, we propose a control structure that exploits these natural inter-joint couplings (Fig. 1).

This control schema contains an ANN module that implements motor synergies in the form of a

feed-forward network (called synergy network in Fig. 1). This module maps 3-D score vectors onto 10-D posture vectors in analogy to Equation 1.

The output of the synergy network can be described by

$$p_j = m_j + \sum_{i=1}^3 w_{ji} s_i \quad (2)$$

where  $w_{ji}$  is the weight matrix which is equivalent to the 3x10 loadings of the PCs and that are used as motor synergies here. The controller compares the target position vector with the current hand position and calculates the score changes necessary to minimize the difference. The result is added to the current 3D score vector, thus updating the arm posture for the next iteration.

We evaluate two different ANN controller variants. The first is a two-layered feed-forward network; the second is a recurrent Elman network (Elman, 1990). Both ANNs are identical except for the additional recurrent connections comprising the context layer of the Elman network (Figure 1).

Owing to the small number of synergies, input and output of the controller are minimal and equidimensional: both the two input position vectors and the output synergy scores are three-dimensional.

The output  $\Delta s$  of the two-layered feed-forward network can be calculated by

$$\Delta s_k = w_{k,n+1}^{out} + \sum_{j=1}^n w_{k,j}^{out} \sigma \left( w_{j,7}^{in} + \sum_{i=1}^6 w_{j,i}^{in} x_i \right) \quad (3)$$

Output of the recurrent Elman network can be calculated by the Equations 4 and 5. First, the intermediate output  $y_h^{hidden}$  at time  $t$  has to be determined by

$$y_h^{hidden}(t) = \sigma \left( w_{j,7}^{in} + \sum_{i=1}^6 w_{j,i}^{in} x_i(t) + \sum_{h=1}^n w_{j,h}^{cont} y_h^{hidden}(t-1) \right) \quad (4)$$

Then, the output  $\Delta s$  at time  $t$  can be calculated according to

$$\Delta s_k(t) = w_{k,n+1}^{out} + \sum_{h=1}^n w_{k,h} y_h^{hidden}(t) \quad (5)$$

The input vector  $\mathbf{x}$  in Eq. 3 and 4 contains the coordinates of the target position,  $\mathbf{tp}$ , and the current hand position,  $\mathbf{cp}$  (see Fig. 1).  $\sigma(x)$  is a hyperbolic tangent function used as sigmoid activation function of the hidden layer.

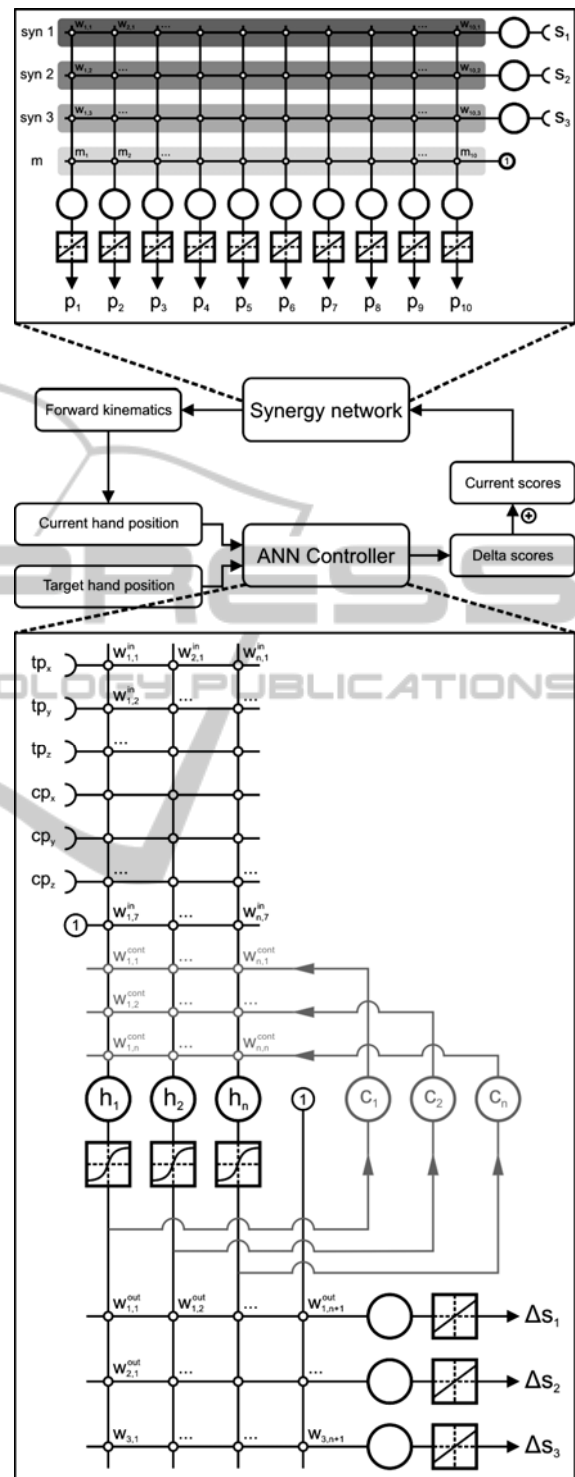


Figure 1: Control schema with inserts showing the synergy network (top insert) and two ANN controller variants (bottom insert). Black structures only: two-layer feed-forward network. Black and gray structures combined: recurrent Elman network. For clarity, the number of hidden units is set to 3 ( $h_1$  to  $h_n$ ).

## 2.4 Network Training

Training data consist of a series of eight goal-directed hand trajectories recorded during experiments in which participants were instructed to catch an approaching ball (Bockemühl, et al., 2010). Each trajectory starts at one of two initial positions, ends at one of sixteen target positions, and contains 25 time steps. Half of the data set (eight trajectories) is used for training, the other half is used for testing generalization (further eight trajectories). In order to account for end-point stability, each trajectory is extended by a leading initial phase of 5 time steps during which the hand remains at the initial position, and a trailing target phase of 10 time steps during which the hand remains at the catching position. In accordance, the target position  $\mathbf{tp}$  is kept at the initial position for 5 time steps and is subsequently set to one of the 16 prospective catching positions for the remaining trial.

The goal of the training is to find weight matrices for the controller ANNs that generate physiologically plausible hand trajectories towards the target. The root mean squared error (RMSE) between training trajectories and generated trajectories was used as the evaluation function. Weight matrix optimization was realized via the Levenberg-Marquardt algorithm (Levenberg, 1944, Marquardt, 1963) implemented in MatLab 7.10 (The Mathworks). To avoid local minima, the training was repeated 100 times, using different randomly initialized weight matrices. As a main objective of this study was to determine the minimal size of the hidden layer, we tested ANNs with 3, 4, 5, 6 or 10 hidden units.

## 3 RESULTS

### 3.1 The Mapping between Synergy Space and Cartesian Space is Bijective

As our movement synergies are principal components of the joint angle space, they describe correlations between joint angles. Owing to the PCA, these synergies are orthogonal to each other. However, the mapping of synergy space into Cartesian space involves non-linear forward kinematics of the controlled arm and, therefore, needs not be bijective: multiple postures, and therefore synergy combinations, could result in the same hand position. A bijective mapping is a

prerequisite for simple control of arbitrary point-to-point movements though. To ensure that the mapping allows arbitrary hand positioning within its working range (surjective mapping) and that any combination of synergies leads to distinct hand positions (injective mapping), Fig. 2 shows the mapping of a 3D grid of synergy combinations into Cartesian space of hand positions. Although the mapping is non-linear, it covers a substantial fraction of the physiological range of a human arm (surjective) and the warped grid in Cartesian space has no overlapping regions (injective).

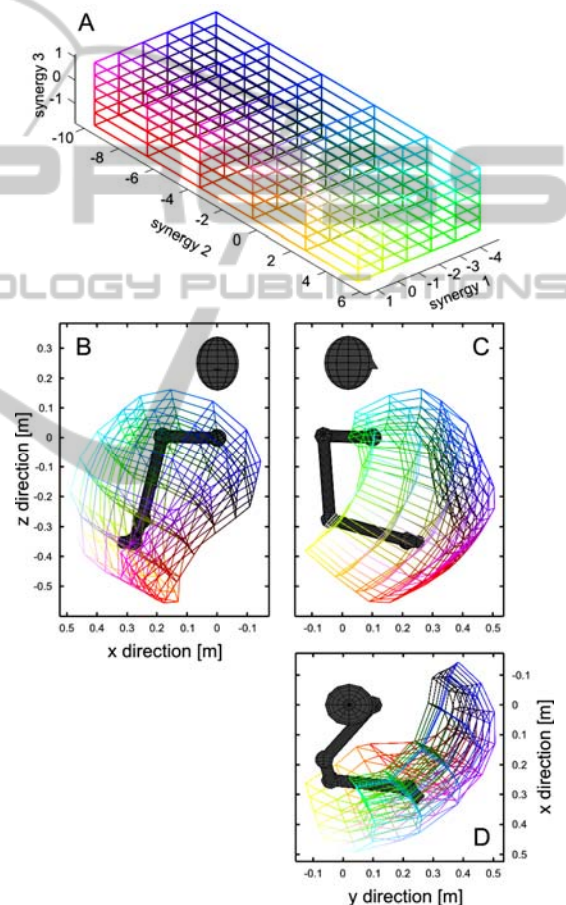


Figure 2: Mapping between synergy space (A) and Cartesian space (B, C and D) of the right human arm. B: Frontal view. C: View from the right. D: Top view. The kinematic model as well as a stylized head are depicted in gray. Colors in synergy space correspond to the equivalent color in Cartesian hand space and vice versa.

### 3.2 Training and Generalization Performance

We find that both controller variants are able to adapt to the training data. Figure 3 shows



representative results for training and generalization performance, using data from a single subject and initial position.

During training, the networks with more than four hidden neurons reached RMSE values of less than 20 mm, regardless of network type. Elman networks with six or more hidden units even reached values as low as 5 mm. However, generalization performance leveled off at hidden layer sizes above 4 units. As generalization is as important as learning performance on trained data, we used 5 hidden units for both controller variants in all other experiments.

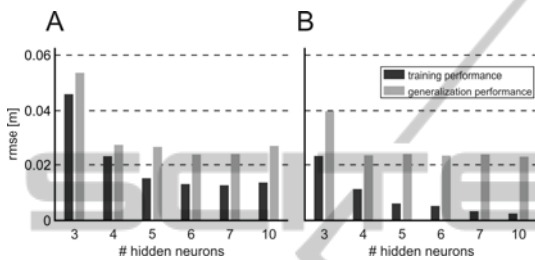


Figure 3: Performance of networks during training and during generalization. A: performance of feed-forward networks. B: performance of recurrent Elman network.

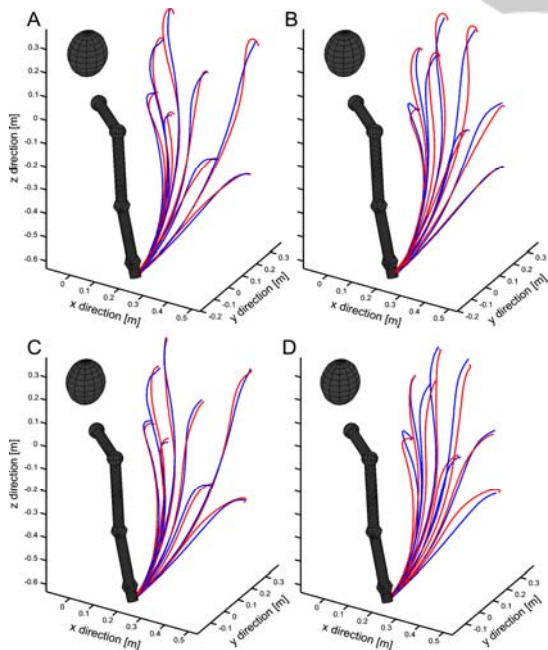


Figure 4: Representative trajectories during 40 time steps generated by a feed-forward network (A and B) and an Elman network (C and D) containing five hidden units. A and C: trajectories to target positions encountered during training. B and D: trajectories to novel target positions. Red: trajectories generated by networks. Blue: trajectories measured during experiment. At the same time, blue trajectories seen in A and C are the training trajectories. View from the rear right side of the kinematic model.

To illustrate overall controller performance, Figure 4 shows representative trajectories produced by a feed-forward network and an Elman network. Whereas trajectories of both controller variants are similar during the first half of the corresponding movements, differences occur toward the end of the trajectory. Here, the feed-forward network produces a small, terminal curvature in the vicinity of the target position. In comparison, the terminal trajectory of the Elman network shows less deviation from the physiological reference data, except for a small but distinct kink near the end.

### 3.3 End-point Stability

An important aspect of target-directed movement is the ability to keep the end-effector at the target after reaching it. We tested this ability of both controller variants by extending the presentation of target inputs by 70 time steps. A representative result is depicted in Figure 5. The prolonged holding phase emphasizes the differences in end-point stability. The feed-forward controller is much better in keeping the end-effector at the target, though the spirals at the end of high trajectories indicate damped oscillations of the posture, beginning with an overshoot followed by a gradual decline towards a stable endpoint. In contrast, the trajectories generated by the Elman controller tend to terminate in a drifting hand position, indicating a constant error output that slowly accumulates. The Elman controller seems not to be able to compensate for errors that occur after the target is reached.

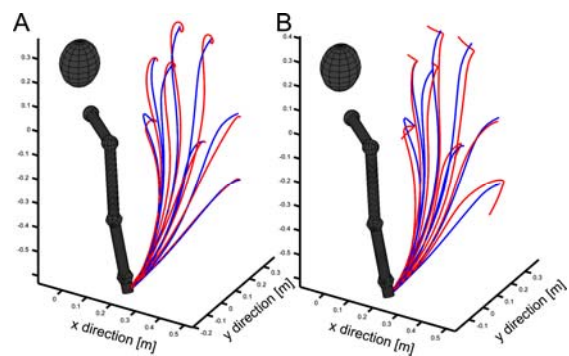


Figure 5: End-point stability. A: Trajectories generated by a feed-forward ANN variant after 110 time steps (see also Fig. 4B). B: Trajectories generated by an Elman ANN variant after 110 time steps (see also Fig. 4D).

## 4 DISCUSSION

We have shown that goal-directed movement of a

human-like limb consisting of arm and shoulder-girdle can be modelled by a comparatively simple closed-loop control schema that comprises small neural network modules and physiological movement synergies.

In classical studies, only artificial or reduced data have been used as a basis for the training of neural networks for motor control (e.g., Massone and Bizzi, 1989, Kawato, et al., 1990, Massone and Myers 1994, Karniel and Inbar, 1997). More recent efforts to model reaching movements based on ANNs do take a physiologically oriented approach (Koike, et al., 2006, Choi, et al., 2009) but still somewhat neglect the importance of motor primitives or synergies.

In contrast, numerous studies find evidence in favor of a modular organization of the nervous system (e.g. Mussa-Ivaldi, et al., 1994, d'Avella, et al., 2006). Although these studies propose potential CNS structures that might be important for motor primitives, these studies often keep silent with regard to more concrete neural models and how exactly movement modules might be combined in a task- or goal-dependent manner in order to produce meaningful behavior.

The approach presented here tries to accommodate both aforementioned aspects: We combine a connectionist approach based on ANNs with experimentally observed movement synergies during a natural reaching task. Combining several DoFs within one synergies and thereby reducing the complexity of the control problem allows us to exploit a bijective mapping between movement synergy space and task space.

Comparative evaluation of the two controllers indicates that, for the present problem, the recurrent Elman network is less appropriate, owing to insufficient end-point stability. Given, that the context layer could be interpreted as an internal model, and that internal models are assumed to be an important computational element central to nervous motor control (Wolpert & Ghahramani, 2000), this is somewhat surprising.

Another notable aspect of the control schema presented here is the low number of necessary neuronal units. A feed-forward network with five hidden units seems to be sufficient for the task of accurately controlling three movement synergies. There are two possible explanations for this: On the one hand, the dissociation of the neuronal substrate into two distinct modules, i.e. into a controller ANN and a synergy network, might be more efficient than a monolithic architecture of similar size. On the other hand, the approach described here is solely

based on joint angle kinematics and neglects a further potential source of complexity: transformation of movement kinematics into a muscle activation pattern. Again, this transformation is a one-to-many mapping and might exacerbate the necessary computations.

## REFERENCES

- Atkeson, C. G., Hollerbach, J. M. (1985). Kinematic features of unrestrained vertical arm movements. *The Journal of Neuroscience* 5, 2318 – 2330.
- Bernstein, N. (1967). The co-ordination and regulation of movements. New York: Pergamon Press Ltd.
- Bockemühl, T., Troje, N. F., and Dürr, V. (2010). Inter-joint coupling and joint angle synergies of human catching movements. *Human Movement Science* 29, 73 – 93.
- Choi, K., Hirose H., Sakurai, Y., Iijima, T., Koike, Y. (2009). Prediction of arm trajectory from the neural activities of the primary motor cortex with modular connectionist architecture. *Neural Networks* 22, 1214 – 1223.
- d'Avella, A., Portone, A., Fernandez, L., Lacquaniti, F. (2006). Control of Fast-Reaching Movements by Muscle Synergy Combinations. *The Journal of Neuroscience* 26, 7791 – 7810.
- Elman, J. L. (1990). Finding Structure in Time. *Cognitive Science* 14, 179 – 211.
- Flash, T., Hochner, B. (2005). Motor primitives in vertebrates and invertebrates. *Current Opinion in Neurobiology* 15, 660 – 666.
- Flash, T., Hogan, N. (1985). The coordination of arm movements: An experimentally confirmed mathematical model. *The Journal of Neuroscience*, 5, 1688 – 1703.
- Karniel A., Inbar G. (1997). A model for learning human reaching movements. *Biological Cybernetics* 77, 173 – 183.
- Kawato, M., Maeda Y., Uno, Y., Suzuki R. (1990). Trajectory formation of arm movement by cascade neural network model based on minimum torque-change criterion. *Biological Cybernetics* 62, 275 – 288.
- Koike, Y., Hirose, H., Sakurai, Y., Iijima, T. (2006). Prediction of arm trajectory from a small number of neuron activities in the primary motor cortex. *Neuroscience Research* 55, 146 – 153.
- Levenberg, K. (1944). A method for the solution of certain nonlinear problems in least squares. *Quarterly Journal of Applied Mathematics* 2, 164 – 168.
- Marquardt, D. W. (1963). An algorithm for least-squares estimation of nonlinear parameters. *Siam Journal on Applied Mathematics* 11, 431 – 441.
- Massone, L., Bizzi, E. (1989). A neural network model for limb trajectory formation. *Biological Cybernetics* 61, 417 – 425.

- Massone, L., Myers, J. (1994). A Neural Network Model of an Anthropomorphic Arm. *IEEE Transactions on Systems, Man, and Cybernetics [B]* 26, 719 – 732.
- Mussa-Ivaldi, F. A., Giszter, S. F., Bizzi, E. (1994). Linear combinations of primitives in vertebrate motor control. *Proceedings of the National Academy of Sciences of the United States of America* 91, 7534 – 7538.
- Ting, L. H., McKay, J. L. (2007). Neuromechanics of muscle synergies for posture and movement. *Current Opinion in Neurobiology*. 17, 622 – 628.
- Todorov, E. (2004). Optimality principles in sensorimotor control. *Nature Neuroscience* 7, 907 – 915.
- Uno, Y., Kawato M., Suzuki R. (1989). Formation and control of optimal trajectory in human multijoint arm movement. *Biological Cybernetics* 61, 89 – 101.
- Wolpert, M., Ghahramani, Z. (2000). Computational principles of movement neuroscience. *Nature Neuroscience* 3, 1212-1217.

